

## Evaluation of Vertical Coherence Length, Twist and Microstrain of GaAs / Si Epilayers Using Modified Williamson-Hall Analysis

Ravi Kumar<sup>1,\*</sup>, Tapas Ganguli<sup>2</sup>, Vijay Chouhan<sup>1,4</sup>, V.K. Dixit<sup>1</sup>, Puspen Mondal<sup>2</sup>, A.K. Srivastava<sup>2</sup>,  
C. Mukherjee<sup>3</sup>, T.K. Sharma<sup>1,†</sup>

<sup>1</sup> Semiconductor Physics & Devices Laboratory, Raja Ramanna Centre for Advanced Technology, Indore - 452013, India

<sup>2</sup> Indus Synchrotron Utilisation Division, Raja Ramanna Centre for Advanced Technology, Indore - 452013, India

<sup>3</sup> Mechanical & Optical Support Section, Raja Ramanna Centre for Advanced Technology, Indore - 452013, India

<sup>4</sup> Currently at High energy accelerator research organization (KEK), Tsukuba 305- 0801, Japan

(Received 05 May 2014; published online 20 June 2014)

Modified Williamson-Hall (WH) analysis is used to determine the reliable values of the microstructures for Zincblende epilayers grown on non-polar substrates. Systematic high resolution X-ray diffraction (HRXRD) experiments are performed for several skew symmetric reflections which enable an accurate measurement of the values of vertical coherence length (VCL) and microstrain of GaAs epilayers grown on Si. Furthermore, a simple method based on the orientation of Burgers vector is proposed for estimating the ratio of tilt and twist. In this method, the twist can be found easily once tilt is known. It is rather quick and the measured values of twist are very similar to those which are otherwise estimated by acquiring numerous HRXRD scans along with tedious fitting procedures. Presence of 60° mixed dislocations is confirmed from the cross sectional high resolution transmission electron microscope images of GaAs / Si samples. Furthermore, the estimated value of VCL is equivalent to the layer thickness measured by the surface profiler.

**Keywords:** HRXRD, GaAs / Si, Anti Phase domain, Microstructure, Williamson-Hall analysis.

PACS numbers: 61.05.cp, 81.05.Ea

### 1. INTRODUCTION

High resolution x-ray diffraction (HRXRD) is widely used in the evaluation of structural parameters of epitaxial layers because of its fast and non-destructive nature. It is known that the Williamson-Hall (WH) analysis is highly effective in evaluating the microstructures of epitaxial and polycrystalline materials [1-3]. Lateral coherence length (LCL), vertical coherence length (VCL), tilt, twist, and microstrain are regularly estimated using WH analysis for many hetero-epitaxial layers, for example in GaAs / Si [3], GaAs / Ge [3, 4], GaP / Si [5], GaN / Sapphire [6, 7], InN / Sapphire [8, 9], and ZnO / Sapphire [10] etc. In WH analysis these structural parameters, usually classified as the microstructures, are determined using a set of symmetric reflections such as (00*l*) and (00.*l*) planes (where *l* = 2, 4, 6) for Zincblende and Wurtzite systems respectively [3, 6-10]. However, in a few cases especially for Zincblende structures WH analysis gives unrealistic information. We recently reported that a modified WH analysis can be very useful under such cases where appropriate values of LCL, tilt and twist are measured without any ambiguity [11]. In case of conventional WH analysis, one needs to record HRXRD patterns for the (00*l*) set of reflections (*l* = 2, 4, 6) where full width at half maximum (FWHM),  $\Delta q_{obs}(\omega / 2\theta)$ , of the diffraction peak in  $\omega / 2\theta$  scans is defined as follows,

$$(\Delta q_{obs}(\omega / 2\theta))^n = (\Delta q_{(00l)VCL})^n + (\varepsilon \times q)^n \quad (1)$$

Where  $\Delta q_{(00l)VCL}$  is the crystal broadening in reciprocal space due to the finite vertical coherence length,  $\varepsilon \times q$

is the broadening due to the microstrain ( $\varepsilon$ ) present in epilayer,  $q$  is the reciprocal space vector, and  $n$  is defined as  $n = 1 + (1 - f)^2$  where  $f$  is the fraction of Lorentzian component in the pseudo-Voigt profile such that the value of  $f$  lies between 0 and 1 [11-13]. In order to obtain the reliable values of  $\Delta q_{(00l)VCL}$  and microstrain a set of at least three parallel reflections are required. For the epitaxial layers grown on (001) nominally oriented cubic substrates, the predominantly allowed reflections are (002), (004) and (006) which is primarily decided by the wavelength of CuK $\alpha_1$  X-ray beam in our HRXRD setup as shown in Fig. 1 [14]. Further higher order symmetric reflections, for example (008), are not accessible using CuK $\alpha_1$  beam as can be understood from Fig. 1. It is therefore obvious that the measured values of microstructure from WH analysis might not be appropriate in case any of the three allowed reflections is adversely affected by the poor signal to noise ratio. Furthermore, one of the allowed reflections, for example (006) in case of GaAs, might be very weak due to minimal contrast in the form factors ( $f$ ) of the constituents atoms. The structure factor ( $s$ ) for ( $hkl$ ) plane of Zincblende structure is given by

$s \propto (f_{III} + f_V e^{-i\frac{\pi}{2}(h+k+l)})$ , where  $f_{III}$  and  $f_V$  are the form factors of the group III and V atoms respectively. In case of GaAs, the values of form factor of Gallium and Arsenic atoms are very close and the contrast further reduces at large diffraction angles [15]. Due to these reasons the value of structure factor for (006) reflection, which is proportional to  $(f_{Ga} - f_{As})$  where  $f_{Ga}$  and  $f_{As}$  are the form factors of Gallium and Arsenic atoms, is going

\* [ravi@rrcat.gov.in](mailto:ravi@rrcat.gov.in)

† [tarun@rrcat.gov.in](mailto:tarun@rrcat.gov.in)

to be very small. Therefore, (006) is a weak reflection in GaAs which leads to poor signal to noise ratio for one of the three symmetric reflections. Hence, WH analysis will provide unrealistic information of the microstructures in case (006) reflections of GaAs is included. Moreover anti-phase domains (APD) are usually generated whenever Zincblende epilayers are grown on non-polar substrates like Si or Ge. Presence of the APD results in selective broadening of some reflections such as (002) and (006) because the structure factor for these reflections depends upon the relative positions of Ga and As atoms [3]. Influence of APD in the selective broadening of a few reflections has also been seen in several other material systems including metallic alloys [3, 5, 16].

Due to the abovementioned reasons, conventional WH analysis is unable to provide reliable values of microstructure for Zincblende epilayers grown on Si substrates. Furthermore, WH analysis cannot be used for evaluating the twist between the mosaic blocks since a set of parallel planes perpendicular to the surface plane is not available in the reflection geometry [11]. Twist is rather evaluated by analyzing various skew symmetric  $\omega$  scans [7, 11, 12]. In view of these limitations, we recently proposed a modified Williamson-Hall analysis in which a set of parallel planes inclined to the surface plane is used [11]. For example, one may use (111), (222), (333) and (444) parallel reflections which lie within the Ewald Sphere for  $\text{CuK}\alpha_1$  X-ray beam as shown in Fig. 1 [14]. Out of these skew symmetric reflections, only (222) is affected by the presence of APD [3]. Therefore, even in the presence of APD, at least three strong reflections such as (111), (333) and (444) are available which can be used to evaluate the microstructure. Note that for (111) and (333) reflections, the structure factor ( $s$ ) is proportion to  $\sqrt{f_{\text{Ga}}^2 + f_{\text{As}}^2}$ , whereas for (444) reflection  $s \propto (f_{\text{Ga}} + f_{\text{As}})$  [15]. By using the modified WH analysis for GaAs epilayers grown on Si substrates, we recently reported realistic values of the LCL, tilt and twist [11]. However, VCL and microstrain parameters are the important constituents of the microstructure of epilayers which were not measured at that time. In this article, the values of VCL and microstrain are reported by using the modified WH analysis. In case of WH analysis, the method for estimating twist is rather cumbersome since one needs to record the diffraction pattern for several skew symmetric reflections. Moreover, one needs to perform an extrapolation procedure for estimating the twist values [7, 11, 12]. Here, we propose a rather simple procedure for estimating the values of twist from the tilt by invoking the Burger vector criteria.

Finally, integration of III-V compound semiconductors with mainstream Silicon (Si) / Germanium (Ge) technology is a very important goal of the semiconductor industry [3-5]. Recently, several successful attempts on the integration of III-V compound semiconductors with mainstream Si, and Ge are reported [5, 17-19]. However, the integration of GaAs based multijunction solar cells on Si requires considerable improvement in the structural quality of grown layers. The major challenge in GaAs / Si integration originates from the 4.1 % lattice mismatch and a large difference in the thermal expansion coefficients [20] which leads to tilt, twist between the mosaic blocks of

grown layer, and a high density of threading dislocations at the interface. The values of microstructures can be evaluated from the modified WH analysis, which can be highly useful in optimizing the structural quality of GaAs / Si heterostructures. Here, the structural parameters of GaAs / Si epilayers are estimated from the proposed WH analysis which are corroborated by the cross sectional high resolution transmission electron microscope (HRTEM) and surface profilometer images.

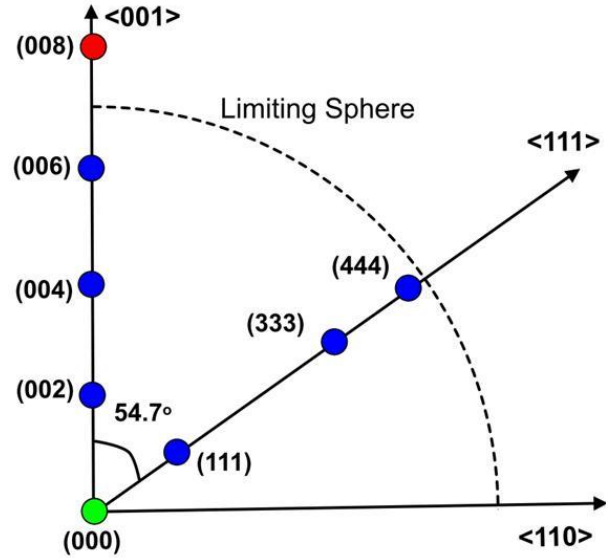


**Fig. 1** – Schematic of the reflection geometry of HRXRD measurements,  $\langle 001 \rangle$  and  $\langle 110 \rangle$  directions are the growth direction and direction lying on the surface respectively. The angle between  $\langle 001 \rangle$  and  $\langle 110 \rangle$  direction is  $54.7^\circ$ . The limiting sphere decided by the wavelength of  $\text{CuK}\alpha_1$  X-ray beam is shown by dotted line. The accessible allowed reflections in HRXRD reflection geometry for  $\text{CuK}\alpha_1$  wavelength are marked by the blue circles. The (008) reflection shown by the red circle is not accessible

## 2. EXPERIMENT

GaAs epilayers are grown by the two-step growth method in a horizontal metal organic vapour phase epitaxy reactor (AIX-200) with a rotating substrate holder at 50 mbar pressure on nominally (001) oriented Si substrates. Trimethyl Gallium and  $\text{AsH}_3$  were used as precursors. Prior to growth, Si substrates were cleaned using a modified RCA cleaning method [10 min in  $\text{H}_2\text{O} : \text{H}_2\text{SO}_4$  (4 : 1) at  $90^\circ\text{C}$ ; 10 min in  $\text{H}_2\text{O} : \text{HCl} : \text{H}_2\text{O}_2$  (5 : 1 : 1) at  $70^\circ\text{C}$ ; 15 s in  $\text{H}_2\text{O} : \text{HF}$  (50 : 1) at room temperature]. A final dilute HF (1 : 70 :: HF :  $\text{H}_2\text{O}$ ) dip was performed right before loading the substrate into the glove box, where Oxygen is kept below 1 ppm, and transferring it to the reactor. Then, Si wafer was preheated at  $870^\circ\text{C}$  for 30 min in a hydrogen ( $\text{H}_2$ ) flow of  $\sim 8$  slpm. This is needed to promote Si surface rearrangement and removal of native oxide from Si substrate. The above procedures for the removal of native oxide from Si wafers are found very successful for the growth of  $\text{Si}_x\text{Ge}_{1-x}$  epilayers on Si substrates [21]. It is reported that following this procedure, the native oxide on Si wafer would not reappear even after 1-2 hour [21]. After pre-heating the Si wafer at  $870^\circ\text{C}$  in presence of  $\text{H}_2$  for 30 min, the temperature was reduced to  $450^\circ\text{C}$  in presence of high flow of Arsine ( $\text{AsH}_3$ ). At this

**Table 1** – Summary of various growth parameters of the three GaAs / Si samples S<sub>1</sub>, S<sub>2</sub> and S<sub>3</sub>

Sample #N <sub>o</sub>	Structure	Growth Temp. (°C)	Thickness (nm)	V / III ratio
S <sub>1</sub>	Nucleating Layer	450	60	337
	Top Layer	650	250	103
S <sub>2</sub>	Nucleating Layer	450	60	518
	Top Layer	670	250	103
S <sub>3</sub>	Nucleating Layer	400	60	337
	Top Layer	670	250	103

temperature, GaAs nucleating layer of thickness ~ 60 nm with V / III ratio ~ 340 was grown. This was followed by the growth of GaAs layer of thickness ~ 250 nm at 650 °C with V / III ratio ~ 100 (Sample S<sub>1</sub>). Similarly by varying the growth temperatures, two more samples (S<sub>2</sub> and S<sub>3</sub>) were also grown to understand qualitatively the influence of growth temperature on the epilayer properties. The growth parameters of three samples are summarized in Table 1.

The thickness of epilayers was determined by a surface profilometer model Alpha-step IQ (KLA Tencor make). Steps on GaAs / Si samples were made by the selective etching of GaAs using CH<sub>3</sub>OH : H<sub>3</sub>PO<sub>4</sub> : H<sub>2</sub>O<sub>2</sub> (3 : 1 : 1) isotropic etch solution [22]. HRXRD experiments were performed using Panalytical X'Pert PRO MRD system. A hybrid monochromator (Goebel's mirror with a four bounce crystal monochromator), which gives CuKα<sub>1</sub> (wavelength, λ = 1.5405 Å) output with a beam divergence of ~ 20 arcsec, was used for making the measurements. A triple axis attachment (also referred to as three bounce collimator) is placed in front of the detector to ensure an acceptance angle of ~ 12 arcsec. It is to be noted that the instrumental broadening is ~ 20 arcsec and the measured widths are at least one order higher than the instrumental broadening. Therefore, the instrumental broadening effects have been neglected in the subsequent data analysis. The measurements were carried out in the symmetric geometry for (00*l*) planes (*l* = 2, 4, 6) and in the skew symmetric geometry for (*lll*) planes (*l* = 1, 3, 4) respectively. The ω/2θ scans, where ω is the angle that the incident X-ray beam makes with the sample surface and 2θ is angle of deviation of the diffracted beam from the incident beam direction, are recorded in the triple axis geometry. The cross sectional HRTEM micrographs are recorded using Philips CM200 at an accelerated voltage of 200 kV. Cross-sectional samples are prepared by the conventional procedures involving mechanical thinning followed by Ar-ion milling.

### 3. THEORETICAL DETAILS

Theoretical details for the determination of LCL, tilt and twist under the modified WH analysis are already reported elsewhere [11]. Here, we discuss the procedure for estimating the values of VCL and microstrain by the modified WH analysis. A simple and quick procedure for estimating the values of twist is also described in the following subsections.

#### 3.1 Vertical Coherence Length and Microstrain Determination

The main mechanism behind broadening of ω/2θ scans is finite VCL and microstrain (ε) present in the

layer. As mentioned earlier, because of the limitations of WH analysis in case of Zincblende layers grown on non-polar (001) substrates, we suggest usage of skew symmetric planes i.e. (111), (333) and (444) reflections in modified WH analysis. The reciprocal lattice vector of these parallel planes is inclined by an angle (ψ = 54.73°) with respect to the surface normal as shown in Fig. 1. To determine the VCL from the modified WH plots using (*lll*) reflection, we use a modified equation which is analogous to the conventional WH equation (1),

$$(\Delta q_{obs}(\omega/2\theta))^n = (\Delta q_{(lll)VCL})^n + (\varepsilon \times q)^n \quad (2)$$

where, Δ*q*<sub>obs</sub>(ω/2θ) is the total broadening of ω/2θ scan in the reciprocal space, and Δ*q*<sub>(*lll*)VCL</sub> is the broadening due to finite VCL in ⟨*lll*⟩ direction. Further, the value of Δ*q*<sub>(*lll*)VCL</sub> is obtained from the intercept of equation 2 while plotting (Δ*q*<sub>obs</sub>(ω/2θ))<sup>n</sup> versus (q)<sup>n</sup> in the modified WH plot for ω/2θ scans. For estimating VCL, one need to consider the fact that (*lll*) planes are inclined to the sample surface at an angle (ψ). We can therefore write the expression of VCL as follows,

$$VCL = \frac{\cos \psi}{\Delta q_{(lll)VCL}} \quad (3)$$

#### 3.2 Twist Determination

In order to estimate the values of twist several ω scans are required for the planes whose angle of inclination with the substrate surface varies from 0° to 90° [11]. The lateral coherence length corrected angular broadening of x-ray peak obtained by ω scan of plane for which ψ = 90° is the value of twist. Since, ω scan for ψ = 90° cannot be recorded in the present reflecting geometry, an extrapolation is carried out as suggested by Lee et al. [7]. The procedure for measuring the values of twist is very laborious and requires adequate modeling [7, 11, 12]. In view of this, we propose a simple and quick procedure for estimating the values of twist for crystalline mosaic blocks. It is generally known that there are two types of dislocations that are prevalent in the lattice mismatched III-V semiconductors : I) pure edge type dislocations with the line of dislocation along [1 - 1 0] and Burgers vector along [1 1 0], II) 60° mixed type of dislocations with the line of dislocation along [1 -1 0] and Burgers vector along [0 - 1 1] direction [15, 23]. Type I dislocations help in relieving the misfit strain and do not contribute to any tilt or twist between the layer and substrate. Burgers vector of a type II dislocation (60° mixed dislocation) can be

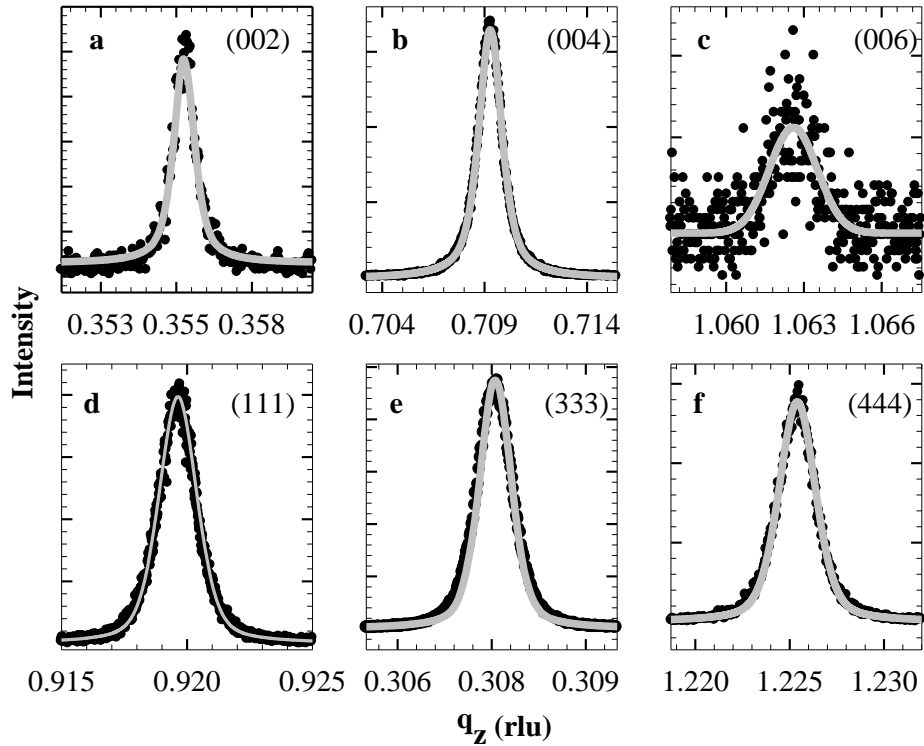


**Fig. 2** – Intensity versus  $q_z$  plot for a: (002), b: (004), c: (006), d: (111), e: (333) and f: (444) reflection of sample  $S_1$  respectively. The overlaying solid lines show the pseudo-Voigt fitting of the experimental data

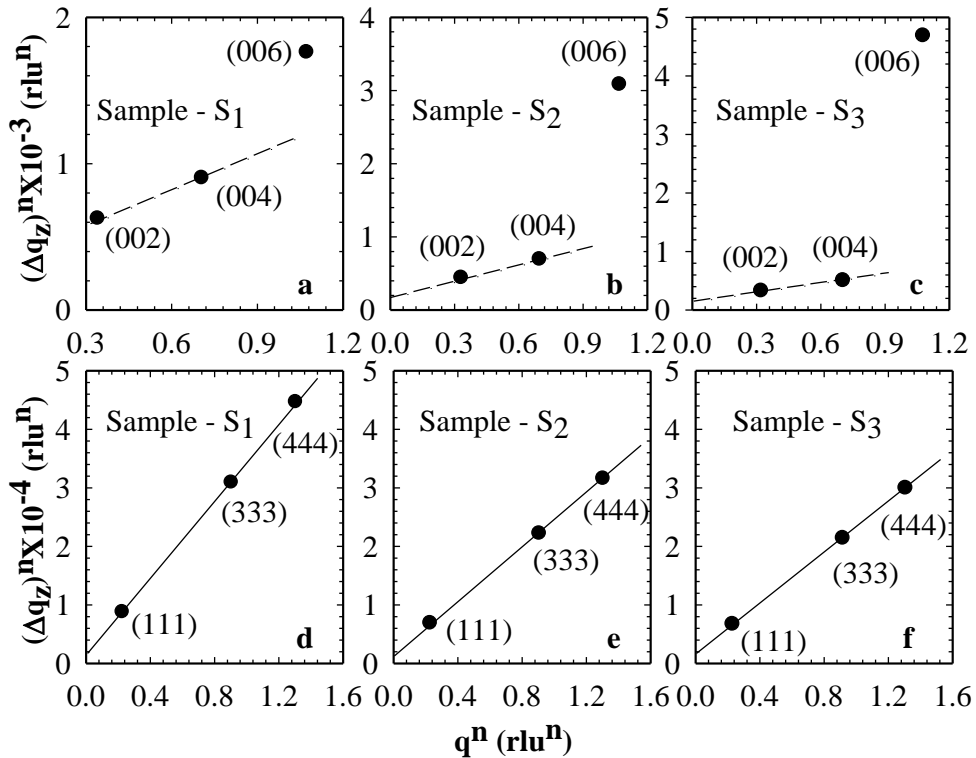


**Fig. 3** – WH plots (a, b, and c) for GaAs / Si samples ( $S_1$ ,  $S_2$ , and  $S_3$ ) using the  $\omega / 2\theta$  scans for a set of symmetric reflections. The dashed straight line is only a guide to the reader's eye. Modified WH plots (d, e and f) for GaAs / Si samples ( $S_1$ ,  $S_2$ , and  $S_3$ ) using the  $\omega / 2\theta$  scans for a set of skew-symmetric reflections. Straight lines show a linear fitting of the experimental data

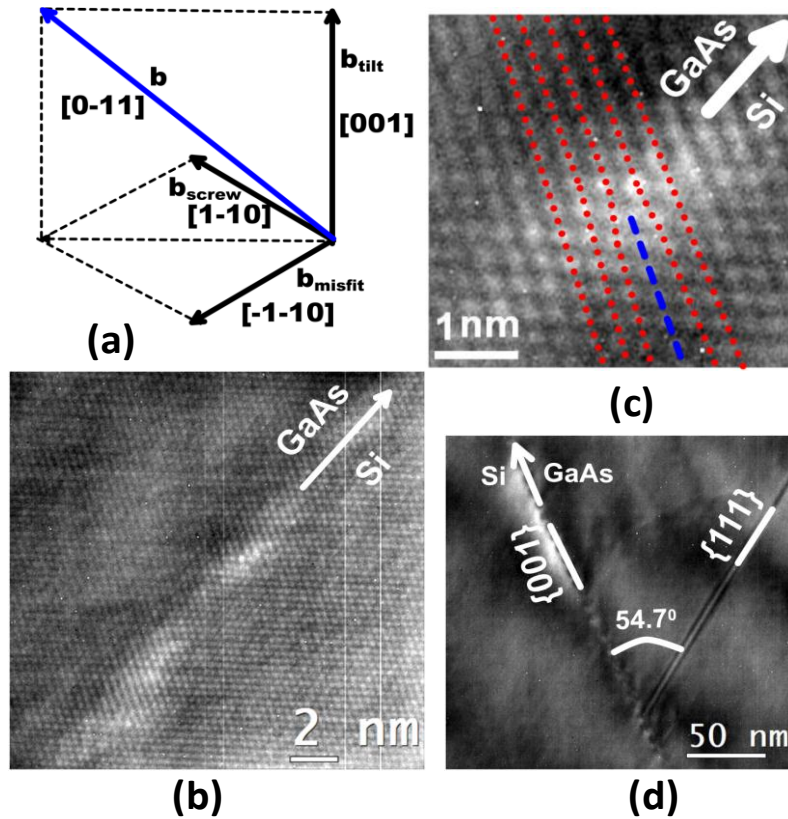


**Fig. 4** – (a) The components of Burgers vector for  $60^\circ$  mixed dislocation, (b) cross section HRTEM image of sample  $S_3$ , (c) magnified HRTEM image around the centre of previous image, and (d) cross section TEM image of samples  $S_3$

**Table 2** – Summary of the microstructure obtained from the modified Williamson-Hall analysis for the three GaAs / Si samples  $S_1$ ,  $S_2$  and  $S_3$ . The value of error bars in the layer thickness, VCL and LCL is  $0.03 \mu\text{m}$

Sample #Ne	Epilayer Thickness ( $\mu\text{m}$ )	VCL ( $\mu\text{m}$ )	Values of tilt (deg.) from our earlier article [11]	Values of twist (deg.) from our earlier article [11]	Twist by Burgers vector consideration (deg.)	Microstrain (%)
$S_1$	0.31	0.30	0.35	0.28	0.25	0.19
$S_2$	0.31	0.34	0.28	0.22	0.20	0.14
$S_3$	0.33	0.35	0.27	0.21	0.19	0.13

decomposed into three parts. For a dislocation line lying along  $[1 - 1 0]$  direction, Burgers vector can be decomposed into the following components as shown in Fig. 4(a):  $(a/2) [0 - 1 1] = (a/4) [-1 - 1 0] + (a/4) [1 - 1 0] + (a/2) [0 0 1] = b_{\text{misfit}} + b_{\text{screw}} + b_{\text{tilt}}$  [15, 23, 24] respectively. The misfit component is responsible for relieving the strain in epilayer. This is identical to the effect of pure edge dislocations (type I dislocation). The screw (twist) component results in a local rotation of the mosaic blocks about the direction resulting in twist between the mosaic blocks and the substrate and also between the individual mosaic blocks. The tilt component results in a tilt between the mosaic blocks and the substrate, and also between the mosaic blocks. It suggests that the tilt and twist in epilayer occur due the presence of a single dislocation line. Magnitude of tilt component and screw (twist) components are  $a/2$  and  $a\sqrt{2}/4$  respectively. The ratio of magnitudes of tilt component and twist component of  $60^\circ$  mixed dislocations is therefore 1.4. Hence, once tilt is measured then the value of twist can be simply estimated by dividing the tilt by a factor of 1.4.

## 4. RESULTS AND DISCUSSION

### 4.1 Determination of VCL and Microstrain in GaAs / Si Epilayers

Figures 2(a-c) show the intensity versus  $q_z$  plots for (002), (004) and (006) reflections of GaAs epilayer for sample  $S_1$ . Note that the plots look similar to those reported earlier [11], however these are recorded following a different procedure ( $\omega/2\theta$  scans) since our main focus is on the estimation of VCL and microstrain. Similar to our earlier observations [11], reflection (006) is very weak and noisy and the fitting is erroneous as obvious from Fig. 2(c).

Figures 2(d-f) show the intensity versus  $q_z$  plots for (111), (333) and (444) reflections of GaAs epilayer of the same sample. The pseudo-Voigt fitting of the curves are shown by the overlaying lines in Fig. 2 [11]. All the skew-symmetric reflections i.e. (111), (333) and (444) are intense and FWHM of all the peaks can be precisely measured. We made similar observations for all the other samples summarized in Table 1. Figures 3(a-c) show the WH plots using the  $\omega/2\theta$  scans of (002), (004)



and (006) reflections for samples S<sub>1</sub>, S<sub>2</sub> and S<sub>3</sub> respectively. Note that the experimental data cannot be fitted by using a straight line as shown in Fig. 3(a-c). It is due to the presence of APDs in the epilayers which results in the broadening of (002) and (006) reflections. Thus, the usage of conventional WH analysis based on (002), (004) and (006) symmetric reflections for measuring VCL is highly inappropriate. Modified WH analysis based on  $\omega/2\theta$  scans of (111), (333) and (444) skew-symmetric reflections is therefore carried out and the results are shown in Figs. 3(d-e). As obvious from Figs. 3(d-e), the experimental data can be accurately fitted with a straight line for all the three samples confirming the usefulness of modified WH analysis for evaluating the microstructures of Zincblende epilayers. Table 2 summarizes the values of VCL and microstrain determined from the modified WH plots for all the samples. The values of VCL obtained for these samples corroborate with the epilayer thickness measured by the surface profiler. The measured values of VCL are thus found to be equivalent to the layer thickness [25-28]. Further, the value of microstrain is smaller for samples having larger VCL as expected. Modified WH analysis based on (111), (333) and (444) reflections is therefore highly useful for evaluating the microstructures of Zincblende epilayers grown on non-polar substrates.

#### 4.2 Determination of Twist Between the Mosaic Blocks of GaAs / Si Epilayers

Figure 4(b) shows the HRTEM image of a large cross sectional area of sample S<sub>3</sub>. In this figure, we find that the interface is not sharp and contains many dislocations. The presence of defect field at the interface is clearly seen in the image. The dislocation type is identified from the cross section HRTEM image. In Fig. 4(c), a small portion around the centre of Fig. 4(b) is magnified to illustrate the arrangement of crystallographic planes. The red dotted lines show the orientation of (111) crystallographic planes. Insertion of an extra half plane along with (111) crystallographic planes clearly confirms the presence of dislocations as shown by the blue dashed line. Burgers vector is inclined from (001) plane confirming that the dislocations are of 60° type [29]. Thus, it is concluded from the HRTEM images that the prevalent dislocations are 60° mixed dislocations present at the interface of GaAs / Si. Similar observations have been made by other researchers for several III-V heterostructure materials [23, 29-31]. Effect of 60° mixed dislocations is clearly observed at the interface of GaAs / Si, where an extended line is observed along  $\langle 111 \rangle$  direction which is inclined at 54.7° from the (001) interface direction as shown in Fig. 4(d). In presence of 60° mixed dislocations, tilt will be equal

to 1.4 times of the value of twist as mentioned in an earlier section of this article. From the reported values of tilt [11], the twist values are calculated for the three samples and are listed in Table 2. Note that the estimated values of twist are in reasonable agreement with those obtained from the modified WH analysis. Therefore, the proposed method of estimating the twist from Burgers vector consideration is acceptable. It totally avoids the requirement of acquiring numerous  $\omega$  scans for different reflections and tedious fitting procedures are not at all needed. Furthermore, it is observed from Tables 1 & 2 that one should choose a lower temperature for the growth of buffer layer since the values of microstrain / tilt / twist are lower for sample S<sub>3</sub> when compared with S<sub>1</sub>. On the other hand, high V / III ratio should be preferred as can be understood by comparing the microstructures of samples S<sub>1</sub> and S<sub>2</sub> from Table 2.

#### 5. CONCLUSION

Conventional WH analysis provides unrealistic information about the vertical coherence length, microstrain and twist of epitaxial and polycrystalline epilayers. Modified Williamson Hall analysis for evaluating the microstructures using skew symmetric (*l*l) reflections (*l* = 1, 3, 4) successfully overcomes these limitations by eliminating the low intensity and selective broadening issues. The estimated values of VCL are in strong corroboration with the values of epilayer thickness / granular size measured by the surface profiler. Furthermore, a straightforward method for estimating the values of twist between the mosaic blocks is proposed. It is based on Burgers vector considerations that totally avoids the requirement of acquiring numerous  $\omega$  scans for different reflections and tedious fitting procedures are not at all needed. Presence of 60° mixed dislocations is clearly observed in cross sectional HRTEM images of GaAs / Si heterostructure. Implementation of modified WH analysis in the evaluation of structural quality of Zincblende epilayers on non-polar substrates should help in the integration of GaAs with mainstream Si technology.

#### ACKNOWLEDGEMENTS

The authors thank Dr. S.D. Singh for help in the planning and growth of the samples, Dr. M.P. Joshi and Dr. Rajmohan for the thickness measurements and Mr. M. Babu for HRTEM sample preparation. The authors also thank Mr. U.K. Ghosh and Mr. A. Khakha for their help during the growth of the samples. Authors also acknowledge Dr. S.M. Oak, Head SSLD, and Dr. P.D. Gupta, Director RRCAT for the constant support during the course of this work.

#### REFERENCES

1. G.K. Williamson, W.H. Hall, *Acta Metallurgica* **1**, 22 (1953).
2. M.J. Hordon, B.L. Averbach, *Acta Metallurgica* **9**, 247 (1961).
3. D.A. Neumann, H. Zabel, R. Fischer, H. Morkoç, *J. Appl. Phys.* **61**, 1023 (1987).
4. C.S. Wong, N.S. Bennett, B. Galiana, P. Tejedor, M. Benedicto, J.M. Molina-Aldareguia, P.J. McNally, *Semicond. Sci. Technol.* **27**, 115012 (2012).
5. V.K. Dixit, T. Ganguli, T.K. Sharma, S.D. Singh, R. Kumar, S. Porwal, P. Tiwari, A. Ingale, S.M. Oak, *J. Cryst. Growth* **310**, 3428 (2008).
6. R. Chierchia, T. Böttcher, H. Heinke, S. Einfeldt, S. Figge, D. Hommel, *J. Appl. Phys.* **93**, 8918 (2003).
7. S.R. Lee, A.M. West, A.A. Allerman, K.E. Waldrip, D.M. Follstaedt, P.P. Proventio, D.D. Koleske, C.R. Abernathy, *Appl. Phys. Lett.* **86**, 241904 (2005).

8. X.L. Zhu, L.W. Guo, N.S. Yu, J.F. Yan, M.Z. Peng, J. Zhang, H.Q. Jia, H. Chen, J.M. Zhou, *J. Cryst. Growth* **306**, 292 (2007).
9. T. Ganguli, A. Kadir, M. Gokhale, R. Kumar, A.P. Shah, B.M. Arora, A. Bhattacharya, *J. Cryst. Growth* **310**, 4942 (2008).
10. S. Singh, T. Ganguli, R. Kumar, R.S. Srinivasa, S.S. Major, *Thin Solid Films* **517**, 661 (2008).
11. R. Kumar, T. Ganguli, V. Chouhan, V.K. Dixit, *J. Nano-Electron. Phys.* **3**, 17 (2011).
12. M.A. Moram, M.E. Vickers, *Rep. Prog. Phys.* **72**, 036502 (2009).
13. V. Srikant, J.S. Speck, D.R. Clarke, *J. Appl. Phys.* **82**, 4286 (1997).
14. M. Birkholz, *Thin Film Analysis by X-Ray Scattering* (WILEY-VCH Verlag GmbH & Co. KGaA: Weinheim: 2006).
15. J.E. Ayers, *Heteroepitaxy of semiconductors: theory, growth, and characterization* (CRC Press: Boca Raton: 2007).
16. B.E. Warren, *X-ray diffraction* (Courier Dover Publications: New York: 1990).
17. A. Beyer, B. Haas, K.I. Gries, K. Werner, M. Luysberg, W. Stolz, K. Volz, *Appl. Phys. Lett.* **103**, 032107 (2013).
18. A. Bondi, C. Cornet, S. Boyer, T.N. Thanh, A. Létoublon, L. Pedesseau, O. Durand, A. Moreac, A. Ponchet, A.L. Corre, J. Even, *Thin Solid Films* **541**, 72 (2013).
19. S. Li, Q. Chen, J. Zhang, H. Chen, W. Xu, H. Xiong, Z. Wu, Y. Fang, C. Chen, *J. Vac. Sci. Technol. B* **31**, 041202 (2013).
20. P. Sheldon, K.M. Jones, M.M. Al-Jassim, B.G. Yacobi, *J. Appl. Phys.* **63**, 5609 (1988).
21. D.J. Meyer, (Academic Press: San Diego, CA: 2001).
22. A. Georgakilas, P. Panayotatos, J. Stoemenos, J.-L. Mourrain, A. Christou, *J. Appl. Phys.* **71**, 2679 (1992).
23. Y. Qiu, M. Li, G. Liu, B. Zhang, Y. Wang, L. Zhao, *J. Cryst. Growth* **308**, 325 (2007).
24. S.G. Tavakoli, O. Hulko, D.A. Thompson, *J. Appl. Phys.* **103**, 103527 (2008).
25. X.L. Wang, D.G. Zhao, X.Y. Li, H.M. Gong, H. Yang, J.W. Liang, *Mater. Lett.* **60**, 3693 (2006).
26. E. Arslan, M.K. Ozturk, A. Teke, S. Ozelik, E. Ozbay, *J. Phys. D: Appl. Phys.* **41**, 155317 (2008).
27. J. Kozłowski, R. Paszkiewicz, M. Tlaczala, *phys. status solidi b* **228**, 415 (2001).
28. B.S. Yadav, S. Singh, T. Ganguli, R. Kumar, S.S. Major, R.S. Srinivasa, *Thin Solid Films* **517**, 488 (2008).
29. T. Soga, T. Jimbo, M. Umeno, *J. Cryst. Growth* **163**, 165 (1996).
30. M. Imai, Y. Miyamura, D. Murata, T. Kanda, T. Kobayashi, K. Omote, *5th International Symposium on Advanced Science and Technology of Silicon Materials* (Hawaii: 2008).
31. A. Vilà, A. Cornet, J.R. Morante, P. Ruterana, M. Loubradou, R. Bonnet, *J. Appl. Phys.* **79**, 676 (1996).